We are IntechOpen, the world's leading publisher of Open Access books Built by scientists, for scientists

4,800
Open access books available

122,000
International authors and editors

135M
Downloads

Our authors are among the

154
Countries delivered to

TOP 1%
most cited scientists

12.2%
Contributors from top 500 universities

CLARIVATE ANALYTICS BOOK CITATION INDEX INDEXED

WEB OF SCIENCE™

Selection of our books indexed in the Book Citation Index in Web of Science™ Core Collection (BKCI)

Interested in publishing with us?
Contact book.department@intechopen.com

Numbers displayed above are based on latest data collected.
For more information visit www.intechopen.com

7

High-Contrast OLEDs with High-Efficiency

Daniel Poitras,† Christophe Py† and Chien-Cheng Kuo‡
†*Institute for Microstructural Sciences, National Research Council of Canada*
1200 Montreal Road, Ottawa K1A 0R6 Canada
‡*Thin Films Technology Center, Department of Optics and Photonics,*
National Central University, 32201 Chung-Li, Taiwan

1. Introduction

As more electronic devices with display are targeted for both indoor and outdoor uses (e.g. cameras, telephones, music players), it becomes increasingly important to solve the problem of contrast of the display under strong external lighting, more particularly under sunlight. In such conditions, the eye has difficulty discriminating the light emitted by the display from the light reflected from the device and surrounding. Increasing the contrast thus consists basically in making sure that the light emitted by the display dominates any other surrounding light reaching the observer. Undesired light from the display itself could be residual light emitted from "*off*" (or dark) pixels, or ambient light reflected on or within the display.

Numerically, the contrast can be expressed as a ratio of the brightest and the darkest elements of a display, taking into account the ambient light reflected by it. In the case of liquid crystal displays, generally with a white backlight source, this contrast is related to the transmittance values of "*on*" and "*off*" pixels (Bahadur, 1991). In the case of light emitting devices, such as organic light emitting displays (OLEDs), the transmittance is replaced by the luminance of the brightest and darkest pixels, and the contrast ratio (CR) is expressed as (Dobrowolski et al., 1992):

$$CR = \frac{L_{on} + R_D L_{ambient}}{L_{off} + R_D L_{ambient}}, \tag{1}$$

where L_{on} and L_{off} are the luminance values of "on" and "off" pixels on the display, respectively, $L_{ambient}$ is the ambient luminance, and R_D is the luminous reflectance of the display, given by

$$R_D = \frac{\int_{\lambda_1}^{\lambda_2} V(\lambda) \cdot R(\lambda) \cdot S(\lambda)\, d\lambda}{\int_{\lambda_1}^{\lambda_2} V(\lambda) \cdot S(\lambda)\, d\lambda}, \quad (2)$$

$V(\lambda)$ being the photopic curve (an eye sensitivity spectrum standard defined by CIE 1931), $R(\lambda)$ is the reflectance of the pixel (*on* or *off*), and $S(\lambda)$ is the source of ambient light [for calculation, CIE standards such as D65 are used (Wyszecki, 1968)]. A value of 20 for CR is usual for a cathode ray tube television in a living room, while a cinema typically has a *CR* of 80 (Poynton, 2003). Care should be taken when comparing CR values as a few different expressions are used to calculate them; for example L_{on}/L_{off} is often used as an expression for *CR*, but should be valid only when the ambient light is sufficiently low, which excludes the cases studied here. Representative luminance values for ambient light and display devices are given in Table I. Without ambient light (i.e. $L_{ambient}$=0 in Eq. 1), *CR* is limited by the darkness of the *off* pixel, which is not as dark for liquid-crystal displays (due to imperfect blocking of its back illumination) as it is for emitting devices (see Table 1). When ambient light is considered, the viewer is seeing the light reflected on the pixels and the only way to prevent it from affecting too much *CR* is to increase the ratio $L_{on}/R_D L_{ambient}$ by (i) increasing L_{on} and (ii) reducing R_D to 1% or less (see Table 2). Thus an ideal display should have a high L_{on}/L_{off} ratio and $L_{on} >> R_D L_{ambient}$.

SOURCE	TYPICAL LUMINANCE L [cd/m²]
Clear day	10^4
Heavily Overcast day	10^2
Bright moonlight	10^{-2}
Moonless overcast night	10^{-4}
CRT	90—150
CRT, "off" pixel	0.01
LCD	400—500
LCD, "off" pixel	0.72
OLED	70—600
OLED, "off" pixel	0

Table 1. Typical values of luminance for different ambient light conditions and display devices (Boff et al., 1988; Anderson, 2005).

R_D [%]	Contrast Ratio *CR*	
	$L_{ambient}$=10^4 cd/m²	$L_{ambient}$=10^2 cd/m²
50	1.1	11
10	1.5	**51**
1.0	6.0	**501**
0.1	**51**	**5001**

Table 2. Values of Contrast Ratio (Eq. 1) corresponding to different values of R_D and $L_{ambient}$ (assuming L_D=500 cd/m²).

In organic light emitting displays (OLEDs), electrons and holes are injected from the cathode and the anode, respectively, to one or several organic layers between them in which they recombine radiatively, resulting in light emission. We distinguish bottom- and top-emission OLEDs, for which emission occurs through a transparent anode/substrate or a semi-transparent cathode, respectively. In most OLEDs, a thick metal layer is encountered as the electrode material on the non-emitting side; the light reflection from such an electrode is high and this results in a low *CR* value. Replacing the metal electrode by a transparent conductor (such as ITO) can contribute to lower the OLED reflectance, but this generally results in a lower carrier injection into the organic layers. For efficient injection, the cathode requires a material with a low work function (such as Ca, Mg:Ag, or Al/LiF), which are all metallic and possess high reflectance. The anode material should have a high work function, and transparent conductors such as ITO are usually the preferred choice for bottom-emitting devices –they obviously don't have high reflectance.

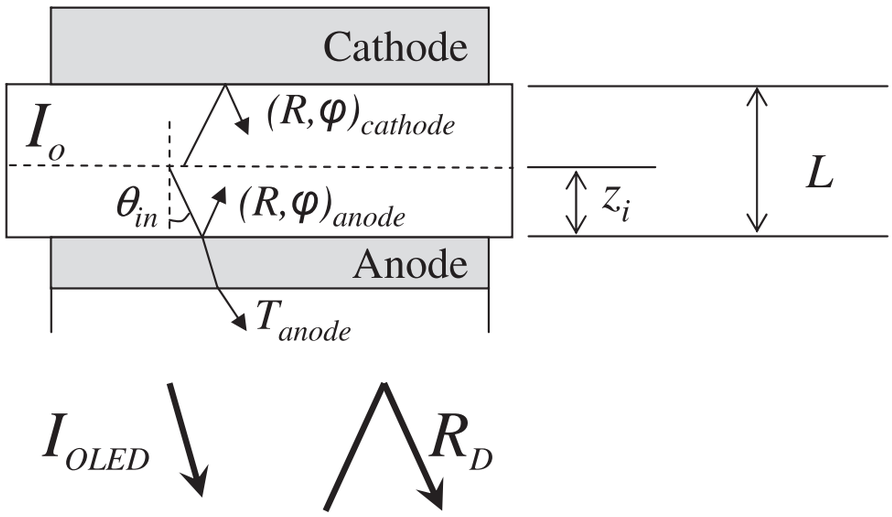

Fig. 1. Schematic view of an OLED showing its Fabry-Perot-like structure and the parameters used in Eq. 3.

2. Theory

2.1 Theory of emission

Several comprehensive models for the emission of dipoles in a multilayer structure have been presented in the literature, which take into account the orientation of dipoles in the emitting layer (Björk, 1991). Less elaborated expressions for the emission of a thin-film structure with an emitting layer can also be developed using an approach similar to the one presented by Smith for describing the transmittance of Fabry-Perot structures, using the concept of effective interfaces (Smith, 1958). We used this approach to obtain the following expression for bottom-emission OLEDs (similar to other expressions that can be found in the literature, for example Lee et al., 2002):

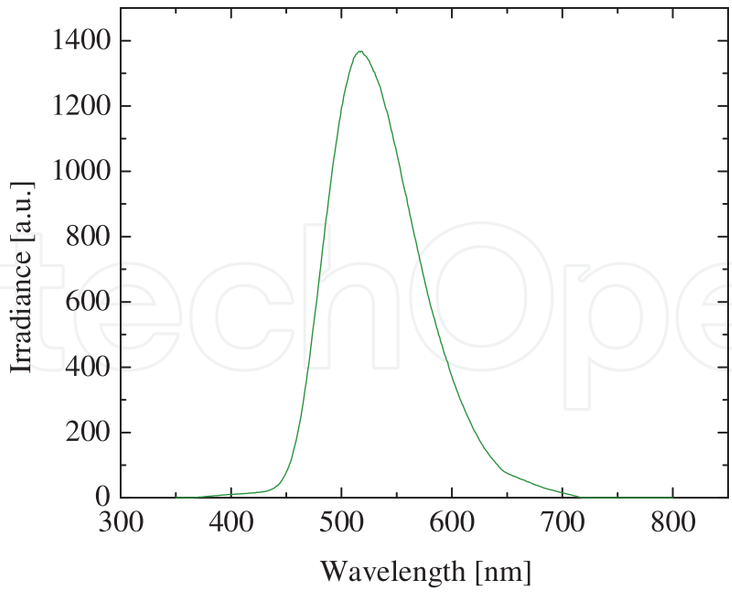

Fig. 2. Emission spectrum of Alq_3. The curve was taken as representing I_0 inside the OLED emitting layer.

$$I_{OLED}(\lambda) = \frac{T_{anode}\frac{1}{N}\sum_{i=1}^{N}\left[1 + R_{cathode} + 2\sqrt{R_{cathode}}\cos\left(\frac{4\pi z_i \cos\theta_{in}}{\lambda} + \phi_{cathode}\right)\right]}{1 + R_{cathode}R_{anode} - 2\sqrt{R_{cathode}R_{anode}}\cos\left(\phi_{cathode} + \phi_{anode} + \frac{4\pi L\cos\theta_{in}}{\lambda}\right)} I_0(\lambda), \quad (3)$$

where R_{anode} and $R_{cathode}$ are the internal reflectance values of the two electrodes, φ_{anode} and $\varphi_{cathode}$ are the phase changes on internal reflection from the mirrors surrounding the cavity layers, T_{anode} is the transmittance of the exit anode, L is the total optical thickness of the cavity layer, $I_0(\lambda)$ is the irradiance of the emitter, $I_{OLED}(\lambda)$ is the irradiance emitted in the glass substrate, z_i is the optical distance between the emitting sublayer i and its interface with the cathode, and θ_{in} is the angle of the emitted beam when measured from inside the emitting material. As shown in Eq. 3, the emitting layer can be divided into N sublayers and their contribution summed up (this step is not essential when the electric field intensity does not change significantly over the emitting layer, as with thin emitting layer, or weak microcavity effect). This equation can include the absorption and the dispersion of the optical constants of the materials. Luminance $L(\lambda)$ spectra can be obtained from Eq. 3 simply by modulating $I_{OLED}(\lambda)$ with the photopic curve. Assuming that the phase conditions in Eq. 3 are optimal, the maximum of emission is obtained approximately when $R_{anode}/(R_{anode}+T_{anode})=R_{cathode}$, which reduces to $R_{anode}=R_{cathode}$ when there is no absorption.

We see that Eq. 3 depends on the internal irradiance $I_0(\lambda)$, which is difficult to determine exactly. In this work, we approximated $I_0(\lambda)$ with the photoluminescence spectra of a thick Alq_3 layer, having a green emission peak (as shown in Figure 2) (Tang, 1987).

As mention above, Eq. 3 is similar to the equation describing the transmittance of a Fabry-Perot, except for the cosine at the numerator. As in Fabry-Perot filters, the multiple internal reflections in OLEDs induce, at some specific wavelengths, a resonance of the light electric-field intensity (or more accurately, the irradiance) distribution inside the OLED.

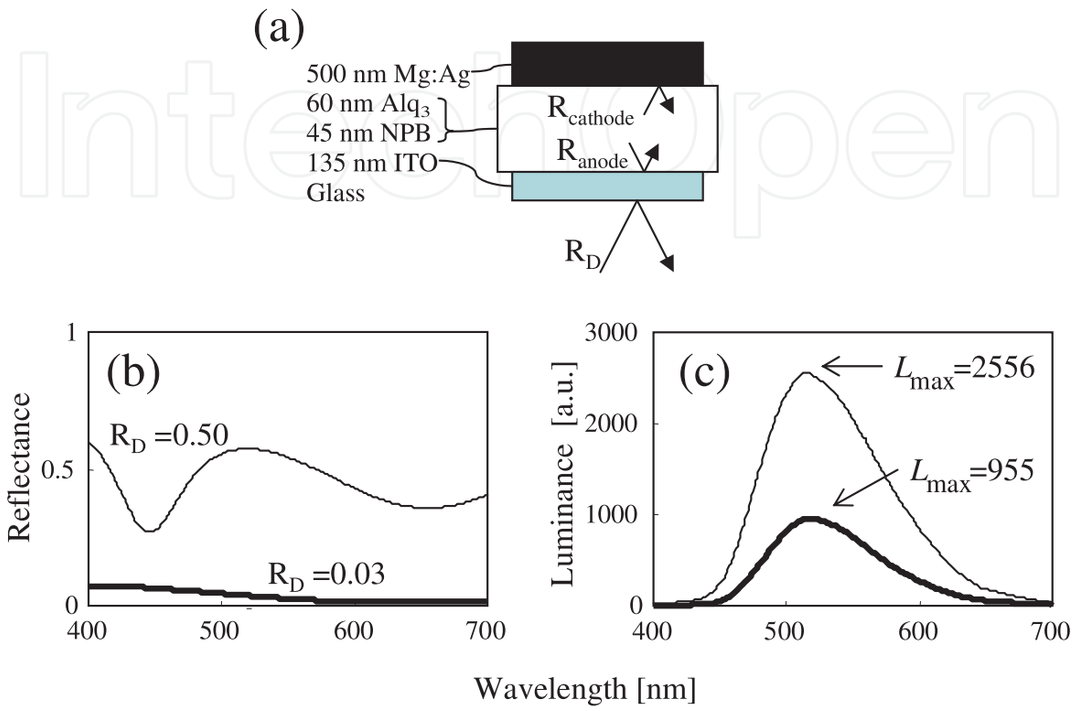

Fig. 3. (a) Schematic representation of a bottom-emitting OLED, (b) Example of reflectance and emission of a conventional OLED (thin line), and one with $R_{cathode}$=0 (thick line). (R_L is the luminous reflectance, given by Eq. 2)

The phenomenon known as "microcavity effect" refers to the enhancement or annihilation of the emitted irradiance related to the position of the emitting material relative to this resonance peak of the irradiance. A weak microcavity effect is usually present in conventional OLEDs because internal reflections are caused by the higher refractive index of the ITO anode compared to most organic layers, and the cathode is highly reflective (Bulovic, 1998). This is usually considered a nuisance, but has been exploited in microcavity OLEDs (Jordan, 1996). With Fabry-Perot filters, the phase condition for the appearance of resonance peaks is given by the following equation:

$$\frac{\phi_{anode} + \phi_{cathode}}{2} - \frac{2\pi cos\theta}{\lambda} = m\pi. \tag{4}$$

For OLEDs, this condition is slightly shifted due to the top cosine term in Eq. 3**.** When all-dielectric mirrors are used, the phase terms φ_{anode} and $\varphi_{cathode}$ can be set to zero; however, when absorbing materials (such as a metal) are used in at least one of the mirrors, the phase terms have to be considered.

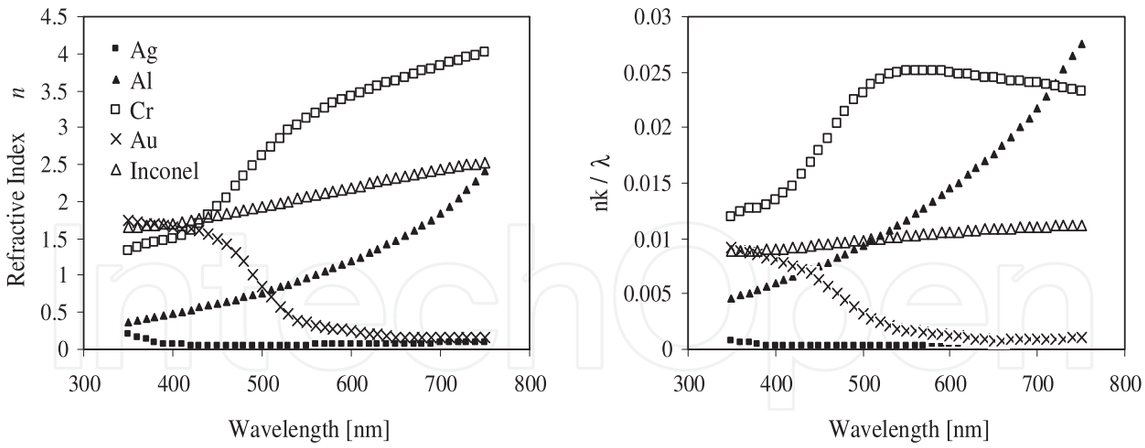

Fig. 4. Refractive index and nk/λ dispersion curves for a few metals.

2.2 Calculation of the reflectance and design

The reflectance of the OLED, R_{OLED}, is calculated using well-know iterative approach for multilayer optics (Macleod, 2001). It is interesting to note that this approach can also be used not only to optimize (minimize) the reflectance of the OLED, but also to simultaneously optimize (maximize) its emission through the optimization of its transmittance (from the substrate towards the cathode), instead of using an exact expression for the emission, such as Eq. 3. It is the comparison of Eq. 3 with the Fabry-Perot equation that makes it possible; the position of the resonance peak in emission is first approximated by Eq. 4 from the Fabry-Perot transmittance peak, and then refined using Eq. 3 to maximize the emission.

3. Review of current approaches for reducing R_D

As seen in Eq. 1 and Table 1, significantly reducing the reflectance of OLEDs is crucial to increase the contrast ratio. Several approaches have been proposed for reaching that goal, which are described briefly in the following paragraphs.

3.1 Use of a polarizer

OLED display manufacturers have so far used circular polarizers borrowed from the LCD technology to improve contrast (Trapani et al., 2003). This approach does not require introduction of new layers in the OLED structure and results in reflectance similar to that of glass. However, polarizers are expensive, generally not flexible, and absorb a substantial amount of the light (up to 40%) (Wu, 2005).

3.2 All-dielectric antireflection coating

Using an all-dielectric antireflection (AR) coatings is the proper way to remove the reflection from the front glass surface when the light is emitted through a glass substrate (bottom-emission).

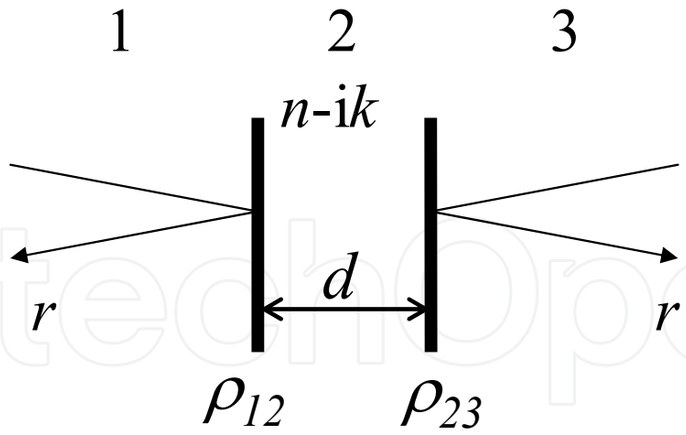

Fig. 5. Schematic view of a metal layer, surrounded by arbitrary materials (ρ_{12} and ρ_{23} can represent the reflection coefficient of multilayers, media 1 and 3 can be different).

However, this AR coating does not remove the reflectance from the OLED structure, on the other side of the glass substrate.

One can also introduce an all-dielectric AR coating in the OLED structure, i.e. between the anode of a bottom-emitting OLED and a glass substrate. Such a coating can have a limited efficiency in reducing R_D when the cathode is a highly reflecting metal (i.e. Al or Mg:Ag). In such cases, metal-dielectric AR coatings can lead to a better performance.

3.3 Scattering Anti-glare surface

One can reduce the specular reflectance of the display by making its top-surface non-planar, an approach that can also enhance the extraction of light from the device. However, the fact that the emitted light is scattered by the surface structure may have a detrimental effect on the resolution of the display (Nuijs & Horikx, 1994).

3.4 Black electrode

In the last few years, many attempts have been made to reduce the reflectance of metal-based electrodes, mainly by making the cathode black (Renault et al., 2000; Krasnov, 2002; Aziz, 2003; Dobrowolski, 1981; Lemarquis & Marchand, 1999) by using absorbing materials in it, or covering it with a conductive black layer coating (similar to the metal-dielectric AR coating described below) (Krasnov, 2002). The result is a reduced reflectance of the OLED sometimes below 1% at the detriment of the emission; or a relatively good emission, but with a higher luminous reflectance (Wu, 2005). Using Eq. 3, we can show that a completely dark cathode (or anode in the case of top emission) is not desired because (i) it does not take into account the contribution to R_D from the other interfaces in the OLED structure, and more important (ii) it destroys any beneficial microcavity effect and reduce the emission, as shown in Fig. 3. In typical OLEDs, a weak microcavity effect is generally present and can be exploited to improve contrast.

3.5 Absorbing Pigments

Absorbing pigments in front of the OLEDs can be used in the fabrication of displays to create red, green and blue (RGB) pixels when combined with a wide band emission OLEDs. These pigments can be used to absorb the light with a wavelength that does not correspond to that of the light emitted by the pixel, thus contributing to reduce the ambient light reflection (Urabe et al., 2004). When combined, these RGB pigments can darken the surfaces surrounding the pixels. The only remaining ambient reflected light is the one corresponding to the wavelength of the '*off*" pixel (e.g. red pixel will reflect red light even when '*off*").

3.6 Metal-dielectric antireflection coating

It has been known for some time that for efficiently reducing the reflectance of highly reflective substrate with a complex admittance (i.e. metals, or coated metals, such as an OLED), it is convenient to use simple metal-dielectric AR coatings similar to those used in black absorbers (Dobrowolski, 1981; Lemarquis & Marchand, 1999) or heat-reflector in solar-cells applications (Macleod, 1978). This type of coatings has been demonstrated for the contrast-enhancement of electroluminescent (EL) displays (Dobrowolski et al., 1992) and on the cathode side of bottom-emitting OLED (see above) (Krasnov, 2002).

4. Our design approach

We mentioned in Secs. 2.1 and 3.4 that keeping a weak microcavity effect is important for maintaining a relatively high emission. When designing the high-contrast OLEDs, our goals are thus (i) to minimize the external R_D of the OLED, and (ii) to maintain R_{anode} and $R_{cathode}$ large enough to keep the emission high. Many of the approaches mentioned above concentrate on darkening the electrode on the non-emitting side of the OLED, neglecting the reflections on emitting side of the OLED and the contribution of the electrodes' reflectance to the efficiency of the OLED. In order to take these aspects into consideration and achieve the goals mentioned above, our approach combines in the OLED structure three types of optical coatings phenomena: antireflection with a metal-dielectric coating on the anode side, microcavity effect at the emitting layer, and an asymmetric reflectance of the anode.

A small microcavity effect, as seen in Sec. 2, is necessary for maintaining a good emission of the device. For that purpose, internal reflections R_{anode} and R_{cathode} must not be reduced to zero, and the organic layers inside the OLED act as cavity layers, so that the position of the emitting layer (the thin recombination layer) must be at a resonance peak of the electric field.

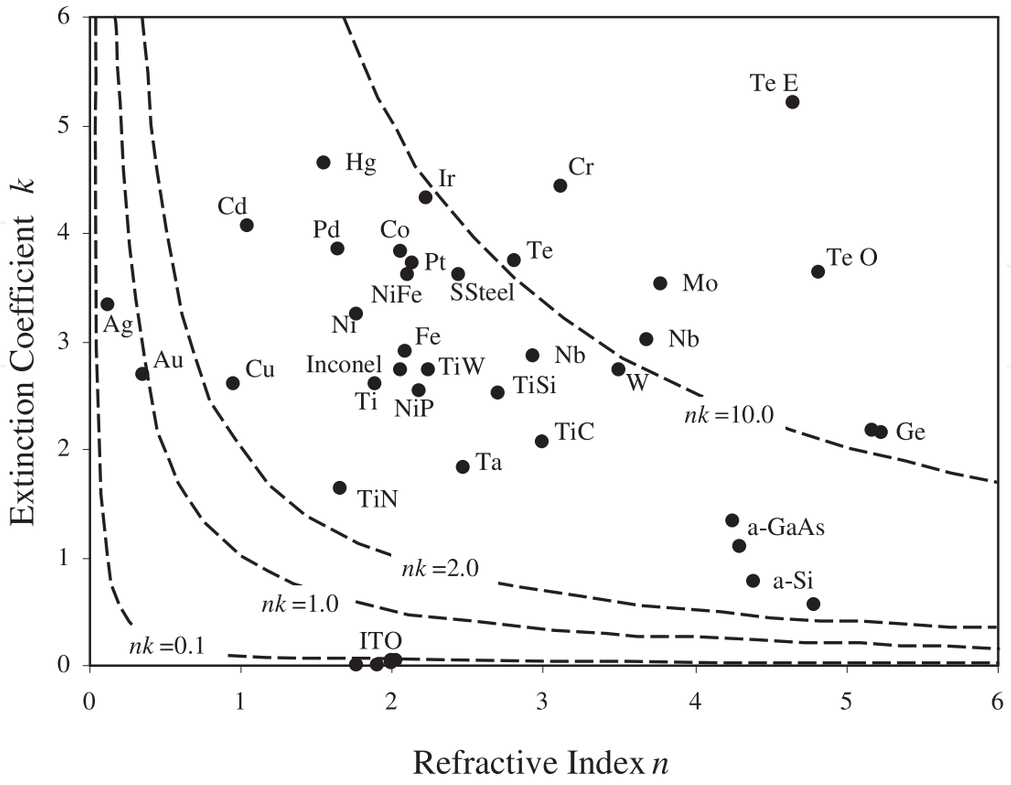

Fig. 6. Refractive indices and extinction coefficients (both given at a wavelength of 550 nm) of several metals and semiconductor materials, as found in the literature. Some isovalue-curves of *nk* product are shown (most optical constants values are extracted from Palik, 1985, and from J.A. Woollam WVASE software, 2009).

As shown in Fig. 1, the combination of good AR coating and small microcavity effect apparently lead to a contradiction of the anode's role: it must have simultaneously a low external reflectance when seen from the substrate and a relatively large internal reflectance when seen from the cavity layers. It has been observed for a long time in thin-film optics that a thin layer of a material with a large extinction coefficient *k* can lead to the kind of asymmetric reflectance (Goos, 1937). In our design, such a layer has thus to be introduced on the anode side of the OLED structure.

Of course, a compromise must still be made between low reflectance and high emission. Also, a too-high microcavity effect is usually not desirable in display application, since it leads to a large dependence of the emission on the angle of view. The key to our design is the asymmetry of the anode internal and external reflection.

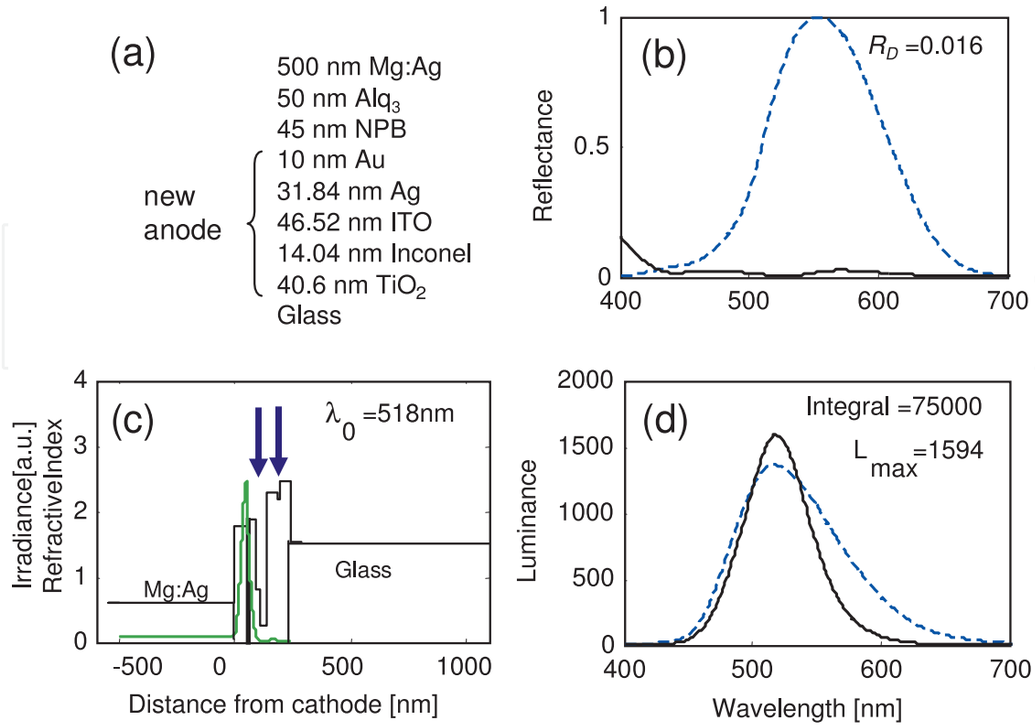

Fig. 7. (a) OLED design; (b) calculated reflectance (solid line) with the photopic curve (dash line) and the value of the luminous reflectance RD; (c) refractive index profile (step) and irradiance profile inside the OLED, with the arrows showing the metal layers, and the emitting layer marked in black.

5. Choice of Materials

5.1 Diode consideration

The selection of materials composing the OLED is important from an electronic point of view. For example, electrode materials must be adequate for carrier injection in organic materials, and they must, along with the organic materials, act as good carrier transport materials. In particular, the cathode must be selected with care, and requires a material with a low work-function to promote injection to an organic layer.

In the present work, we choose well-known materials for the OLED "core" layers: Mg:Ag as a cathode (electron injection) material, Alq3 for the electron transport and emitting layer, NPB simultaneously as a electron-blocking and hole-transport layer (to ensure that electrons and holes recombine in Alq3). Given the low mobility of organic materials, it is also important that their thickness be close to the diffusion length of the charges they transport; this usually constraints the optical design since the resulting thickness of the organic stack is somewhat less than a half-wavelength. In some cases, ITO was used for the anode (hole injection) material. The other materials included in the design are mentioned in the following sub-sections.

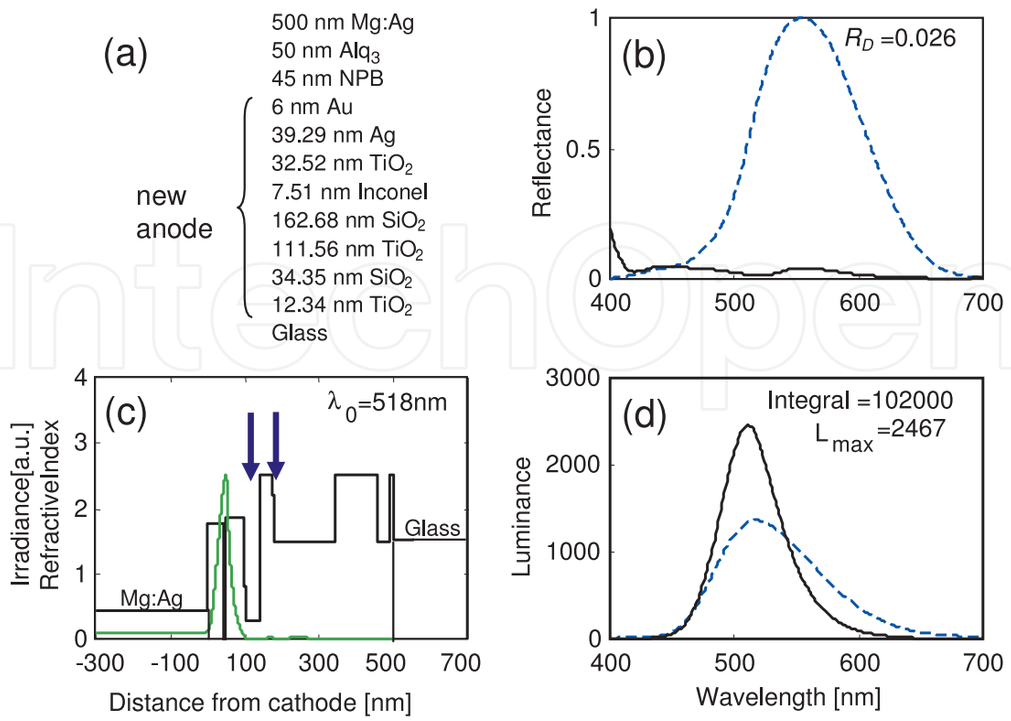

Fig. 8. (a) OLED design; (b) calculated reflectance (solid line) with the photopic curve (dash line) and the value of the luminous reflectance R_D; (c) refractive index profile (step) and irradiance profile inside the OLED, with the arrows showing the metal layers, and the emitting layer marked in black.

5.2 Optical consideration, metal-dielectric antireflection coating

In metal-dielectric AR coatings, the main role of the metal layers is not to absorb the light but to benefit from its complex admittance n-ik in order to more efficiently reach to AR condition (Lemarquis & Marchand, 1999). For that reason, metals with relatively large k are required for this type of coatings (see Fig. 6). Metals that are highly reflecting, such as metals with $n < 1$, are usually avoided. In addition, metals with n that decreases with decreasing λ (often called "abnormal dispersion") are needed to compensate for the increase of optical thickness in the dielectrics at shorter wavelengths. This type of optical constants dispersion is also needed so that the metal does not introduce chromatic absorption in the device, which requires a constant nk/λ for all the wavelengths of interest. Figure 4 shows n and nk/λ dispersion curves for several metals. Chromium is often used for metal-dielectric black absorbers, but our preferred choice is Inconel (an alloy of Cr:Ni:Fe), which is less absorbing and has a very flat nk/λ curve.

5.3 Optical consideration, electrode with asymmetric reflection

As mentioned in Sec. 4, a material with $k > 0$ is required at the anode to maintain a cavity effect in the OLED while reducing its external reflectance, i.e. introducing an asymmetry of the internal and external reflectance of the anode. The optical constants required for that

purpose can be found by looking at the reflection coefficients r and r' from both side of an arbitrary layer, with arbitrary interfaces (they could include multilayer), as shown in Fig. 5:

$$r = \frac{\rho_{12} + \rho_{23} exp(-2i\beta)}{1 + \rho_{12}\rho_{23} exp(-2i\beta)}, \qquad r' = \frac{\rho_{23} + \rho_{12} exp(-2i\beta)}{1 + \rho_{12}\rho_{23} exp(-2i\beta)}, \tag{5}$$

with $\beta = \frac{2\pi}{\lambda}\tilde{n}dcos\theta = \frac{2\pi}{\lambda}(n - ik)dcos\theta.$

Clearly, the exponential term differentiates r and r'. It can be shown from Eq. 5 that a large k value is essential to increase the asymmetry in reflectance, with a sufficiently large thickness d; a large n value will also increase the asymmetry, but is not essential. In the case of the anode (as in many other cases involving asymmetric reflectance), a reduction of the light absorption in the layer is important. The irradiance absorbed by a layer is given by the following relation (Macleod, 2001):

$$I_{abs} = \frac{2\pi}{\lambda} nkd\left|E\right|^2 \gamma, \tag{6}$$

where E is the average amplitude of the electric field in the film considered and γ is the free space admittance (a constant). From this equation, we see that reducing the thickness and the amplitude of the electric field inside the layer will lead to a low absorption. This can be done when refining the design of the OLED. Equation 6 also indicates that materials with a low nk product will lead to lower absorption. Figure 6 shows the optical constants of many absorbing materials, and help to find materials having the required (i) high k value and (ii) low nk value. We see on Figure 6 that semiconductor materials (Ge, GaAs, and Si) have relatively low k values and large nk products, while ITO has a low nk product, but also a low k. Metals, on the other hand, have larger k values, but most of them are too absorbing (large nk product). Only silver (Ag) and gold (Au), two transition metals, have a suitably low n value and large k value; they are the preferred choice for our application.

6. Application to high-contrast OLED

6.1 Examples of design

We used the ideas presented in the previous Section and optimized the layers thicknesses of OLED structures consisting of thick-Mg:Ag|organics|Au/Ag|ITO|metal-dielectric-AR|glass in order to reduce R_D, while keeping $R_{cathode}$ and R_{anode} sufficiently high for maintaining a weak cavity effect.

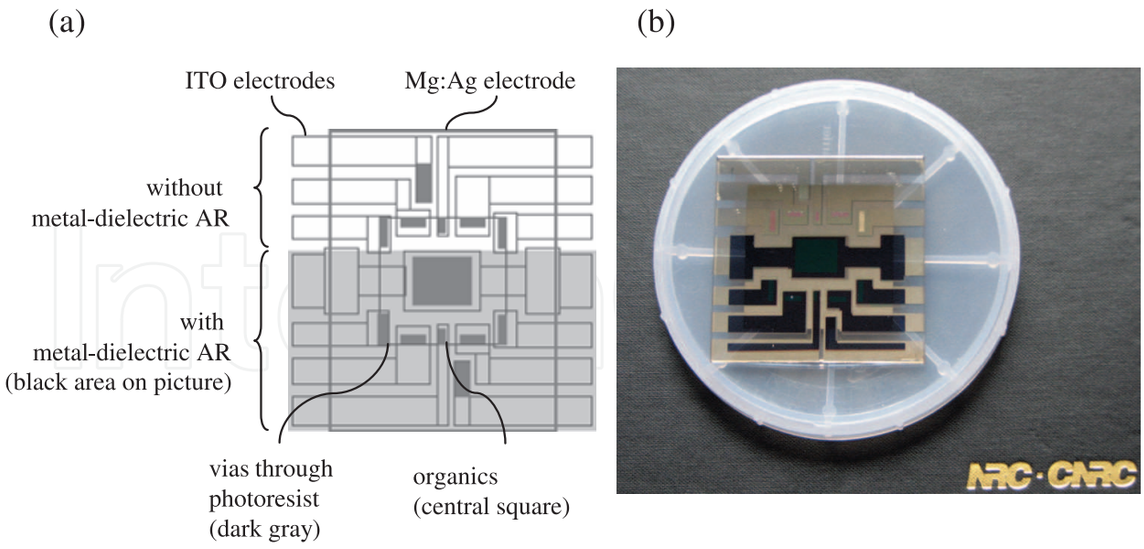

Fig. 9. (a) Schematic bottom view of multi-segment OLED device with and without metal-dielectric AR. (b) Picture of such a device after fabrication. This device corresponds to the design presented in Figure 8.

During theses optimizations, it was important to constrain the thickness values of organic materials to ensure high efficiency OLEDs. For a similar reason, we introduced an Au layer (which has a higher work function than Ag) to facilitate hole injection in the hole transport layer (see Sec. 7). In addition, the thickness of the ITO film had to be large enough to form a low resistivity anode and facilitate the contact with an external lead (although in some cases, we found that the Au/Ag layer was thick enough so that no ITO layer was required).

Figures 7 and 8 show two different designs with a different number of layers in the metal-dielectric AR part of the structure, along with their calculated performances (reflectance and luminance spectra). The complex refractive index of all layers were measured from films deposited in the same conditions as our devices. When compared to the performance of a conventional OLED shown in Fig. 3(b) and (c), we see that the new designs reduce the reflectance to 2% and less, which is 25 times less than that of a typical OLED, and that the emission is of the same order of magnitude.

Figure 7(c) and 8(c) also show the distribution of the irradiance inside the OLEDs at the peak wavelength. The maximum of irradiance at the position of the emitting layer indicates that a microcavity effect occurs in the OLED. Not shown here is the fact that the optimization of such designs with absorbing layers involves the adjustment of phase values φ_{anode} and $\varphi_{cathode}$ in Eq. 3 (Poitras et al., 2003). In addition, the reduced irradiance values at positions corresponding to the metal layers contribute to reduce the absorption of emitted light in these layers (see Eq. 6).

6.2 Example of actual device

SiO_2, TiO_2 and Inconel were deposited in a dual ion-beam sputtering deposition chamber (Spector, Veeco-IonTech), and all other materials were thermally evaporated in a high-vacuum cluster tool (Kurt J. Lesker), in separate chambers for metals and organics to avoid cross-contamination and interface degradation. The complex refractive index spectra of individual films were derived from measurements by ex-situ variable-angle spectroscopic ellipsometer (VASE, J.A. Woollam Co.). These spectra were used to produce the final design described and simulated in Figure 8.

The profile of the calculated irradiance, which is the light radiant flux per unit area, is shown in Figure 1 at the peak wavelength of emission. The cavity is designed so that the irradiance has a maximum in the Alq_3 layer at the NPB interface, where the emission originates, and a minimum in the Ag/Au absorbing bilayer, where light absorption is reduced. High contrast is obtained because the Au/Ag bilayer is highly absorbing seen from the outside. Using published extinction coefficients for evaporated Au and Ag films (AIP, 1972), the transmittance of the Au/Ag bilayer without the cavity effect is calculated to be 0.042.

Actual devices were fabricated with the DBR materials sputtered through a shadow mask on only half of a 2x2 in^2 glass slide to provide direct comparison between filtered and unfiltered sides (see Figure 9). Ag and Au were evaporated through a shadow-mask to define electrode tracks and an electrical separator lithographically patterned to define diode segments (Roth et al., 2001). NPB, Alq_3, Mg:Ag and a Ag capping layer were evaporated with the contacts masked off. The samples were not encapsulated.

Reflectance measurements were performed using a spectrophotometer (Lambda-19, Perkin-Elmer) equipped with a reflectance accessory (with an angle of incidence of 7°). The values obtained (see Figure 10) are in qualitative agreement with our simulation, and show a very clear improvement of the contrast. The spectral shift and discrepancy in values of reflectance between simulated and measured spectra is due to the cumulative error in film thicknesses, most probably from organic materials for which the control is less precise, but also from variations in the optical constants of metallic films, which are critical.

The unfiltered OLED shows a deep absorption peak due to the Fabry-Perot resonance of the naturally-occurring weak microcavity, and the filtered OLED shows oscillations in the reflectance due to the same effect. Lower reflectance filters could be designed with more layers in the DBR, at the expense of added complexity.

7. Conclusion

It is conceivable that future outdoor displays will combine different approaches: intensity control, microstructure for light extraction, or displays based on reflection might be used, but they will certainly include reflection-suppressing designs. As we saw earlier, efficiently suppressing the light reflection from the device requires an integration of the antireflection layers with the entire display device.

We have demonstrated the concept of a multilayer anode comprising an Au/Ag bilayer and a metal-dielectric AR coating that has both a high internal reflectance and a low outside reflectance. The former property is used to maintain a microcavity effect in the OLED that is tuned to maximize light out-coupling, and the latter to improve the OLED contrast ratio.

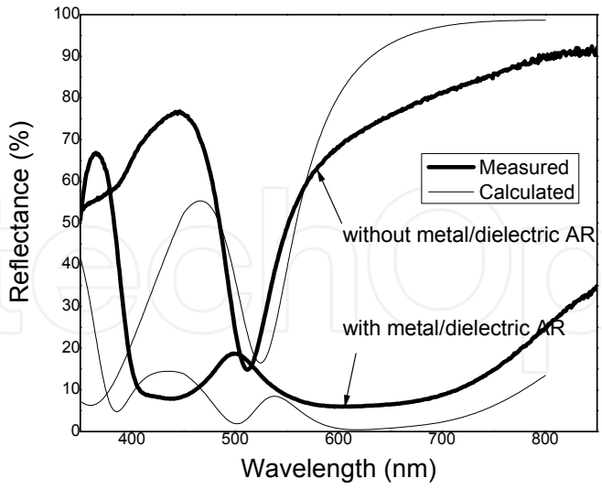

Fig. 10. Theoretical and measured reflectance spectra, for OLED with and without integrated metal-dielectric layers.

Further designs are being considered with varying thicknesses of the Au/Ag layer, and fewer layers in the metal-dielectric coating for a simpler fabrication process.
Although the basic concepts described concerning the microcavity effect have been applied in the present work to bottom-emission OLEDs and specific materials only, they are general and will remain true whatever the materials used in the device (i.e. polymer-based), and for other device structures (such as top-emitting-OLED, tandem-OLED, etc.).
The problem of contrast is complex: the optimum contrast for which a viewer is comfortable depends on the color, and the surrounding light. For outside application, ideal solutions will probably involve not only the reduction of the reflectance of the display, such as explained here, but also the adjustment of display luminance and correction for the gamma parameter (Poynton, 1993; Devlin et al., 2006).

Acknowledgments

The authors wish to thank Hiroshi Fukutani, Eric Estwick and Xiaoshu Tong for their technical assistance. We also are grateful to Dr. Ye Tao for many fruitful discussions, and to Prof. C.C. Lee.
Parts of this work were presented at the OSA 2007 Optical Interference Coating Conference (Tucson, June 2007) and at the 13th Canadian Semiconductor Technology Conference (Montreal, August 2007).

8. References

AIP (1972) *American Institute of Physics Hanbook*, Gray, D.E. ed. McGraw-Hill, 3rd edition, ISBN 978-0070014855, New York.

Anderson, P. (2005). *Advance Display Technologies*, JISC Technology & Standards Watch Report, August 2005. http://www.jisc.ac.uk/whatwedo/services/services_techwatch/techwatch/techwatch_reports_0503.aspx

Aziz, H.; Liew, Y.-F.; Grandin, H. M. & Popovic, Z. D. (2003). Reduced reflectance cathode for organic light-emitting devices using metalorganic mixtures, *Appl. Phys. Lett.* Vol. 83, pp. 186—188.

Bahadur, B. (1991). Display parameters and requirements, In: *Liquid Crystals: Applications and Uses*, B. Bahadur (Ed.), p. 82, World Scientific, ISBN 978-981-02-0111-1, Singapore.

Björk, G. (1991). Modification of spontaneous emission rate in planar dielectric microcavity structures, Physical Review A, Vol. 44, No. 1, pp. 669—681.

Boff, K.R.; Lincoln, J.E. & Armstrong, H.G. (1988). *Engineering Data Compendium. Vol.1. Human Perception and Performance*, Aerospace Medical Research Laboratory, Wright-Patterson Air Force Base, ISBN 978-9992149201, Ohio.

Bulovic, V.; Khalfin, V.B; Gu, G.; Burrows, P.E.; Garbuzov, D.Z. & Forrest, S.R. (1998). Weak microcavity effects in organic light-emitting devices, *Phys. Rev. B.* Vol. 58, No. 7, p. 3730.

Devlin, K.; Chalmers, A. & Reinhard, E. (2006). Visual calibration and correction for ambient illumination, *ACM Transactions on Applied Perception.* Vol. 3, No. 4, pp. 429—452.

Dobrowolski, J.A. (1981). Versatile computer program for absorbing optical thin film systems, *Appl. Opt.* Vol. 20, pp. 74-81.

Dobrowolski, J.A.; Sullivan, B.T. & Bajcar, R.C. (1992). Optical interference, contrast-enhanced electroluminescent device. *Applied Optics*, Vol. 31, No. 28, pp. 5988—5996, ISSN 0003-6935.

Goos, F. (1937). Durchlässigkeit und reflexionsvermögen dünner silberschichten von ultrarot bis ultraviolet, *Zeitschrift für Physik A Hadrons and Nuclei.* Vol. 106, No. 9—10, pp. 606—619.

Jordan, R.H.; Rothberg, L.J.; Dodabalapur, A. & Slusher, R.E. (1996). "Efficiency-enhancement of microcavity organic light-emitting diodes, *Appl. Phys. Lett.* Vol. 69, No. 14, p. 1997.

Krasnov, A. N. (2002). High-contrast organic light-emitting diodes on flexible substrates, *Appl. Phys. Lett.* Vol. 80, pp. 3853—3855.

Lemarquis, F. & Marchand, G. (1999). Analytical achromatic design of metal-dielectric absorbers, *Appl. Opt.* Vol. 38, pp. 4876—4884.

Lee, G.J.; Jung, B. Y.; Hwangbo, C. K. & Yoon, J. S. (2002). Photoluminescence characteristics in metal-distributed feedback-mirror microcavity containing luminescent polymer and filler, *Jpn. J. Appl. Phys.* Vol. 41, p. 5241.

Macleod, H.A. (1978). A new approach in the design of metal-dielectric thin-film optical coatings, *Optica Acta.* Vol. 25, No. 2, pp. 93—106.

Macleod, H.A. (2001). *Thin-Film Optical Filters*, Institute of Physics Publishing, ISBN 0750306882, Bristol.

Nuijs, A. M. & Horikx, J. J. L. (1994). Diffraction and scattering at antiglare structures for display devices, *Appl. Opt.* Vol. 33, No. 18, pp. 4058—4068.

Palik, E. D. (1985). *Handbook of Optical Constants of Solids, Vols. I and II,* Academic Press, ISBN 0125444222, New York.

Poitras, D.; Dalacu, D.; Liu, X.; Lefebvre, J.; Poole, P.J. & Williams, R. L. (2003). Luminescent devices with symmetrical and asymmetrical microcavity structures, *Proceedings of the 46th Annual Tech. Conf. of Society of Vacuum Coaters,* pp. 317—322, Philadelphia, May 2003, ISSN 0737-5921, SVC Publication, Albuquerque.

Poynton, C.A. (1993). 'Gamma' and its Disguises: The Nonlinear Mappings of Intensity in Perception, CRTs, Film and Video, *SMPFTE Journal,* Vol. 102, No. 12, pp. 1099—1108.

Poynton, C.A. (2003). *Digital video and HDTV – algorithms and interfaces*, Morgan Kaufmann Publisher, ISBN 1558607927, San Francisco.

Py, C.; Poitras, D.; Kuo, C.-C. & Fukutani, H. (2008). High-contrast Organic Light Emitting Diodes with a partially absorbing anode, *Opt. Lett.* Vol. 33, No. 10, pp. 1126—1128.

Renault, O.; Salata, O. V.; Etchells, M.; Dobson, P. J. & Christou, V. (2000). A low reflectivity multilayer cathode for organic light-emitting diodes, *Thin Solid Films*, Vol. 379, pp. 195—198.

Roth, D.; Py, C.; Fukutani, H.; Marshall, P.; Popela, M. & Leong, D. (2001). An Organic Digital Integrated Multiplexing Clock Display, *Presented at the 10th Canadian Semiconductor Technology Conference, Ottawa, Canada, Aug 13—17.*

Smith, S.D. (1958). Design of multilayer filters by considering two effective interfaces, *J. Opt. Soc. Am.* Vol. 48, No. 1, pp. 43—50.

Tang, C.W. & VanSlyke, S.A. (1987) Organic electroluminescent diodes, *Appl. Phys. Lett.* Vol. 51, No. 11, pp. 913--915.

Trapani, G.; Pawlak, R.; Carlson, G. R. & Gordon, J. N. (2003). High durability circular polarizer for use with emissive displays, US Patent 6549335.

Uriba, T.; Yamada, J.; Sasaoka, T. (2004) Display and method of manufacturing the same, US Patent 2004/0147200A1.

Wu, C.-C.; Chen, C.-W.; Lin, C.-L. & Yang, C.-J. (2005) Advanced Organic Light-Emitting Devices for Enhancing Display Performances, J. Display Technol. Vol. 1, No. 2, pp. 248—266.

Wyszecki, G. (1968). Recent Agreements Reached by the Colorimetry Committee of the Commission Internationale de l'Eclairage (abstract). , *J. Opt. Soc. Am.* Vol. 58, No. 2, pp. 290—292.

WVASE32 software (J.A. Woollam Co., Lincolrn NE)

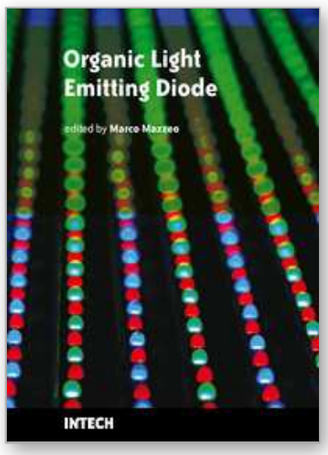

Organic Light Emitting Diode

Edited by Marco Mazzeo

ISBN 978-953-307-140-4
Hard cover, 224 pages
Publisher Sciyo
Published online 18, August, 2010
Published in print edition August, 2010

Organic light emitting diodes (OLEDs) have attracted enormous attention in the recent years because of their potential for flat panel displays and solid state lighting. This potential lies in the amazing flexibility offered by the synthesis of new organic compounds and by low-cost fabrication techniques, making these devices very promising for the market. The idea that flexible devices will replace standard objects such as television screens and lighting sources opens, indeed, a new scenario, where the research is very exciting and multidisciplinary. The aim of the present book is to give a comprehensive and up-to-date collection of contributions from leading experts in OLEDs. The subjects cover fields ranging from molecular and nanomaterials, used to increase the efficiency of the devices, to new technological perspectives in the realization of structures for high contrast organic displays and low-cost organic white light sources. The volume therefore presents a wide survey on the status and relevant trends in OLEDs research, thus being of interest to anyone active in this field. In addition, the present volume could also be used as a state-of-the-art introduction for young scientists.

INTECH
open science | open minds

InTech Europe
University Campus STeP Ri
Slavka Krautzeka 83/A
51000 Rijeka, Croatia
Phone: +385 (51) 770 447
Fax: +385 (51) 686 166
www.intechopen.com

InTech China
Unit 405, Office Block, Hotel Equatorial Shanghai
No.65, Yan An Road (West), Shanghai, 200040, China
中国上海市延安西路65号上海国际贵都大饭店办公楼405单元
Phone: +86-21-62489820
Fax: +86-21-62489821

IntechOpen